ELSEVIER

Ceramics International 31 (2005) 655–661

CERAMICS INTERNATIONAL

www.elsevier.com/locate/ceramint

Crack suppression behavior with post-process parameters in $BaTiO_3$-based Ni-MLCCs

Dong-Ho Park[a], Yeon-Gil Jung[a,*], Ungyu Paik[b]

[a]*Department of Ceramic Science and Engineering, Changwon National University, #9 Sarim-dong, Changwon, Kyungnam 641-773, Korea*
[b]*Department of Ceramic Materials Engineering, Hanyang University, #17 Haengdang-dong, Seongdong-gu, Seoul 133-791, Korea*

Received 14 June 2004; received in revised form 30 June 2004; accepted 10 August 2004
Available online 10 December 2004

Abstract

Effects of post-process parameters, such as temperature, holding time, and pressure direction, on crack evolution are investigated in $BaTiO_3$-based multilayer ceramic capacitors (MLCCs), showing X7R characteristic. Vickers indentation is conducted at each plane of the MLCCs before and after the post-process. Crack evolution in the MLCCs is definitely suppressed through the post-process. Difference of crack length between directions at same plane is also reduced through the post-process. The minimum crack length after the post-process is 19 ± 4 μm and 12 ± 5 μm at the x plane, 23 ± 7 μm and 13 ± 3 μm at the y plane, and 14 ± 2 μm and 19 ± 8 μm at the z plane in the parallel and perpendicular directions to the electrode, respectively. Holding time in the post-process with width direction affects the crack formation within an error range, showing shorter crack length in perpendicular direction rather than in parallel direction to the electrode. Higher temperature, 900 °C, is relatively more effective in reducing crack length than lower temperature, 600 °C, especially at the x plane. The post-process with width direction for the x and z planes and length direction for the y plane is more useful for reducing crack length or suppressing crack propagation.

Keywords: C. Mechanical properties; D. $BaTiO_3$ and titanates; E. Capacitors; Post-process

1. Introduction

Progress in multilayer ceramic capacitors (MLCCs) fabricating technology has been driven by the need to increase capacitance while at the time maintaining product reliability and lowering production costs. For high capacitance in MLCCs, reducing of the active thickness is a much more effective strategy for increasing volume efficiency than increasing of the dielectric constant alone. For this purpose, the key approach is reducing the thickness of the dielectric layer using fine-grained $BaTiO_3$ [1]. However, increasing the number of the active layer gives other problems due to the difference of density and thermal expansion coefficient between inner and outside regions (margins) with and without the electrode, respectively, resulting in structural defects and crooked shape of MLCCs. Usually these disadvantages with multi-lamination in MLCCs can create residual stresses during the firing process, causing delamination and cracks during manufacturing and/or thermomechanical service. Therefore, the release of the residual stresses and the control of the structural defects, including the estimation and understanding of the residual stresses induced on MLCCs, are one of the key technologies in increasing the reliability and lifetime of MLCCs [2–6].

The residual stresses created at the margins of MLCCs due to the difference in shrinkage of each direction and in the thermal expansion coefficient between dielectric and electrode layers have been evaluated using a sharp indentation method in our previous study [7]. In which the residual stresses are dependent on the direction to lamination and electrode. A method to control and/or release the residual stresses in $BaTiO_3$-based Ni-MLCCs

* Corresponding author. Tel.: +82 55 279 7622; fax: +82 55 262 6486.
E-mail address: jungyg@changwon.ac.kr (Y.-G. Jung).

0272-8842/$30.00
doi:10.1016/j.ceramint.2004.08.003

of X7R characteristic has been proposed in the other previous study, using pressure and heat treatment [8]. In the post-process using pressure and heat treatment, even though the residual tensile stresses, dangerous component for crack formation and reliability, are changed to the residual compressive stress and the residual compressive stresses are enhanced, the role of parameters in the post-process is not discussed. Therefore, it will be useful to have a precise control of parameters in the post-process for improving reliability of MLCCs.

In the present work, the effects of holding time, heat treatment temperature, and pressure direction on crack formation and/or suppression behavior in MLCCs are investigated in order to optimize the post-process. The influences of direction to the electrode and distance from the electrode on the crack evolution are extensively observed as well.

2. Experimental procedure

MLCCs samples used in this study are commercial products showing X7R characteristic. The dimensions of MLCCs specimens are 3 mm × 2 mm × 1.6 mm with 330 active layers including the cover layer (margins) of ≈250 μm, and the thickness of the dielectric and electrode layers are ≈3 μm and ≈2 μm, respectively.

The MLCCs were packed with ZrO_2 powder and put into a graphite die, and then were heat-treated at 600 °C and 900 °C, 30 MPa in each direction [with width (*y* direction) or length (*x* direction) direction, as shown in Fig. 1] with different holding times of 1 min, 2 min, and 4 min under vacuum (0.1 Torr). The schematic diagram representing the pressure direction and experimental concept for the post-process is shown in Fig. 1.

The polished specimens for indentation were prepared by grinding to 10 μm finish and subsequently polished to 1 μm. To remove residual stresses during grinding and polishing, the MLCCs were re-polished with SiO_2 colloid sol of 10 nm. Selected polished surfaces were gold-coated and examined by optical microscopy (EPIPHON, Nikon, Japan) and scanning electron microscopy (SEM, S2700, Hitachi, Japan).

In this present study, all indentations were made on the margins of MLCCs with a microhardness tester (Mitutoyo, AVK-C2, Japan) using a diamond Vickers shaped indentor, considering only effects of the direction to the lamination or the electrode, and the distance from the electrode. The schematic diagram of Fig. 1 shows the indentation site for measurement of the crack length after indentation with the load of 0.5 N. The indenter dimension and crack length were measured using optical microscopy and SEM.

3. Results and discussion

The effect of holding time at 900 °C in the post-process through the width direction on crack length is shown in Fig. 2, as a function of the distance from the electrode. The heat treatment temperature of 900 °C was selected by considering the post-annealing temperature of MLCCs (950 °C). When the post-process is performed with the holding time of 1 min, the crack length at the *x*–*z* plane (hereinafter *x* plane as shown in Fig. 1) is reduced to 19 ± 4 μm in the parallel direction to the electrode (hereinafter *x* direction as shown in Fig. 1) and to 14 ± 4 μm in the perpendicular direction (hereinafter *z* direction as shown in Fig. 1), showing the effect of the holding time in the *x* direction. The crack length before the post-process is 35 ± 6 μm and 18 ± 3 μm in the *x* and *z* directions at the *x* plane, respectively. However, the holding time does not affect the crack length at the *y*–*z* planes parallel and perpendicular to the electrode (hereinafter *y* and *z* planes as shown in Fig. 1, respectively), showing a little scattering in the crack length. The crack length is not dependent on the distance from the electrode. The crack

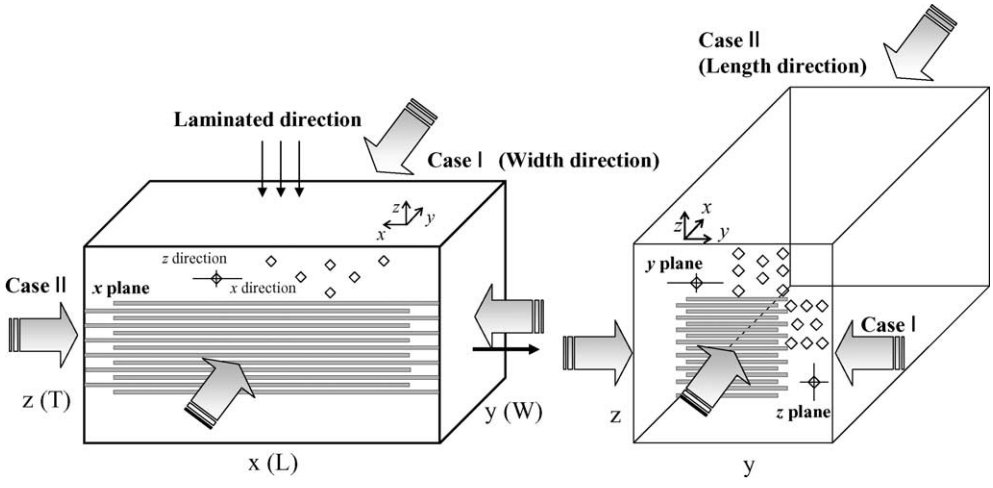

Fig. 1. Schematic diagram of pressure direction in post-process and indentation site for measurement of crack length in MLCCs.

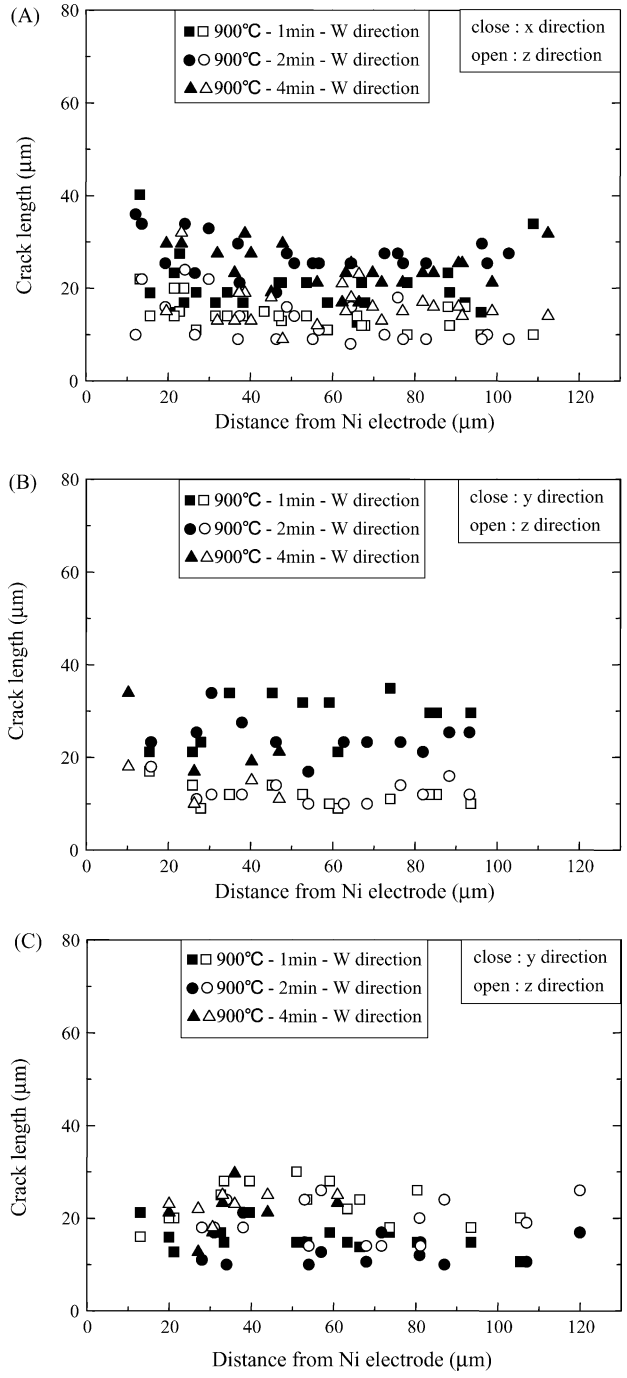

Fig. 2. Crack length at each plane dependent on holding time in post-process through width direction at 900 °C, as a function of distance from electrode: (A) *x* plane, (B) *y* plane, and (C) *z* plane.

length in each direction at each plane after the post-process is summarized in Table 1 with the holding time, including the crack length before the post-process. The crack length is not affected by the holding time except for the *x* direction at the *x* plane.

The effect of heat treatment temperature in the post-process through the width and length directions on crack length is shown in Figs. 3 and 4, respectively, in the case of the holding time of 1 min. Also, the crack length at 600 °C is compared with that at 900 °C in Table 2. Temperature does not affect crack length except for the *x* direction at the *x* plane, showing the unbalance of the crack length depending on the direction to the electrode. The effect of pressure direction and temperature in the post-process on the crack evolution can be more clearly observed by comparing the difference between crack lengths created in each direction parallel (hereinafter *x* direction at the *x* plane and *y* direction at the *y* and *z* planes) and perpendicular (hereinafter *z* direction at all planes) to the electrode, as shown in Figs. 5 and 6. The difference in crack length in each direction parallel and perpendicular to the electrode means that there is the stress unbalance with the direction. The stress

Table 1
Crack length in each direction and plane with different holding time after post-process at 900 °C through width direction and before post-process

Plane and direction	Holding time		
	1 min	2 min	3 min
x plane, after			
x direction (μm)	19 ± 4	27 ± 4	24 ± 6
z direction (μm)	14 ± 4	13 ± 7	16 ± 6
Before			
x direction (μm)	35 ± 6		
z direction (μm)	18 ± 3		
y plane, after			
y direction (μm)	27 ± 6	24 ± 3	23 ± 7
z direction (μm)	13 ± 7	13 ± 3	14 ± 4
Before			
y direction (μm)	40 ± 7		
z direction (μm)	19 ± 3		
z plane, after			
y direction (μm)	16 ± 4	14 ± 3	21 ± 8
z direction (μm)	23 ± 4	20 ± 5	23 ± 4
Before			
y direction (μm)	18 ± 3		
z direction (μm)	33 ± 10		

Table 2
Crack length in each direction and plane with pressure direction after post-process at 900 °C and 600 °C for holding time of 1 min

Plane and direction	Conditions			
	900 °C		600 °C	
	Width (μm)	Length (μm)	Width (μm)	Length (μm)
x plane				
x direction	19 ± 4	27 ± 4	28 ± 7	23 ± 4
z direction	14 ± 4	14 ± 3	14 ± 4	12 ± 5
y plane				
y direction	27 ± 6	26 ± 3	27 ± 5	25 ± 3
z direction	13 ± 7	15 ± 3	14 ± 4	14 ± 2
z plane				
y direction	16 ± 4	15 ± 2	15 ± 4	14 ± 2
z direction	23 ± 4	24 ± 4	19 ± 8	24 ± 2

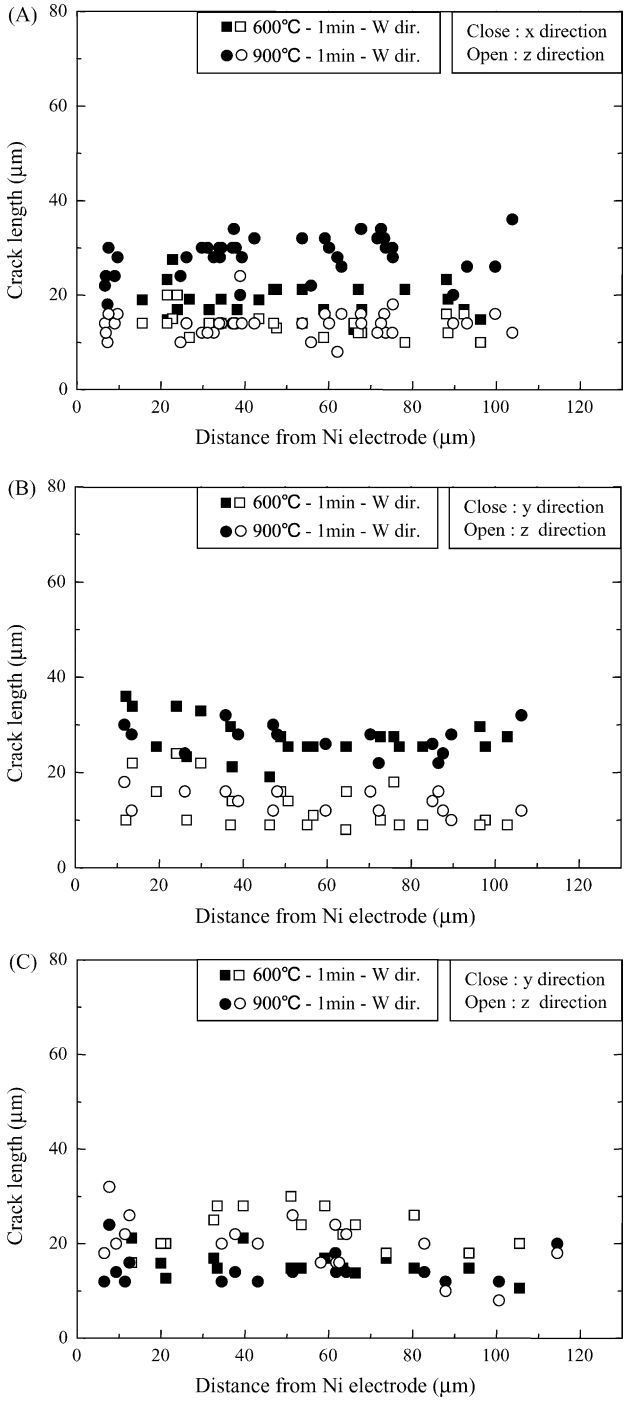

Fig. 3. Crack length with heat treatment temperature, 600 °C and 900 °C, in post-process through width direction, as a function of distance from electrode: (A) *x* plane, (B) *y* plane, and (C) *z* plane.

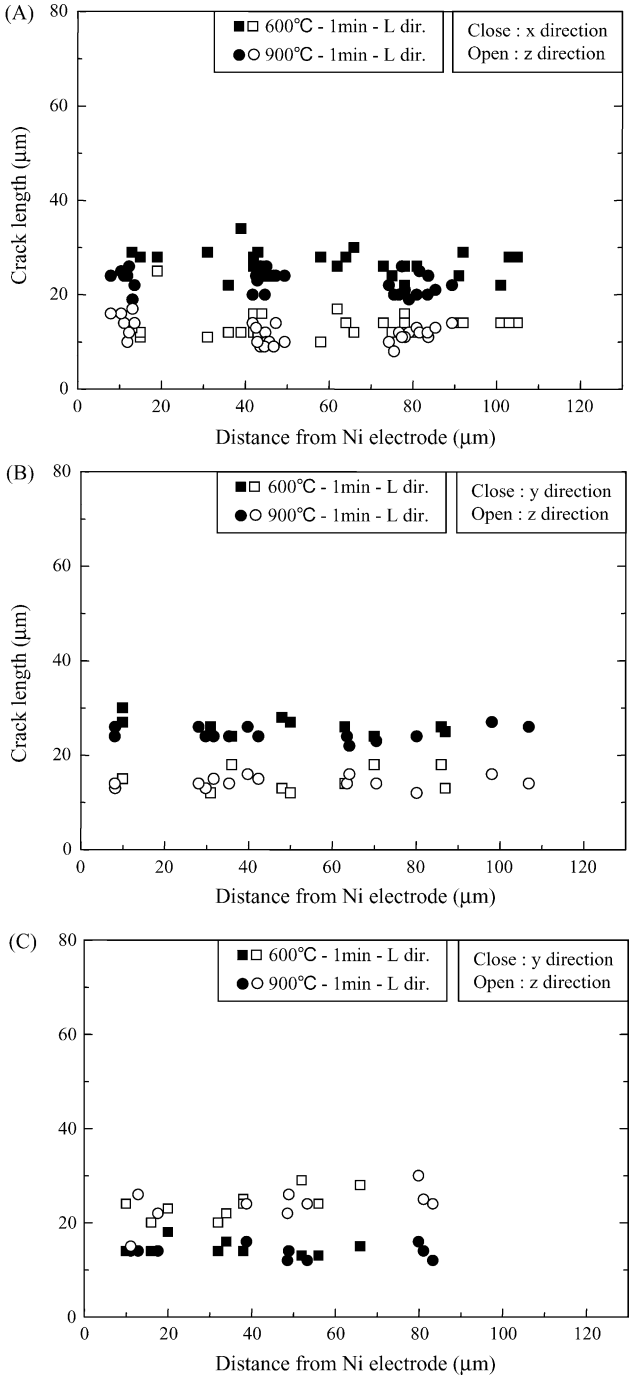

Fig. 4. Crack length with heat treatment temperature, 600 °C and 900 °C, in post-process through length direction, as a function of distance from electrode: (A) *x* plane, (B) *y* plane, and (C) *z* plane.

unbalance could be reduced by the post-process, which is expected with the crack suppression as previous mentioned.

When the post-process is performed through the width direction at 900 °C (Fig. 5), the crack lengths in the *x* and *z* directions at the *x* plane are similar to each other, showing the difference of 5 ± 5 μm in the crack length in each direction. However, the post-process through the length direction indicates the difference of 13 ± 9 μm. This means that the stress unbalance disappears through the width direction, but still appears through the length direction, even though the difference decreases compared to the value of 17 ± 5 μm before the post-process. The difference also decreases after the post-process at the *y* and *z* planes without the effect of the pressure direction. The difference of 21 ± 8 μm at the *y* plane and -15 ± 11 μm at the *z* plane before the post-process is reduced to 12 ± 5 μm and

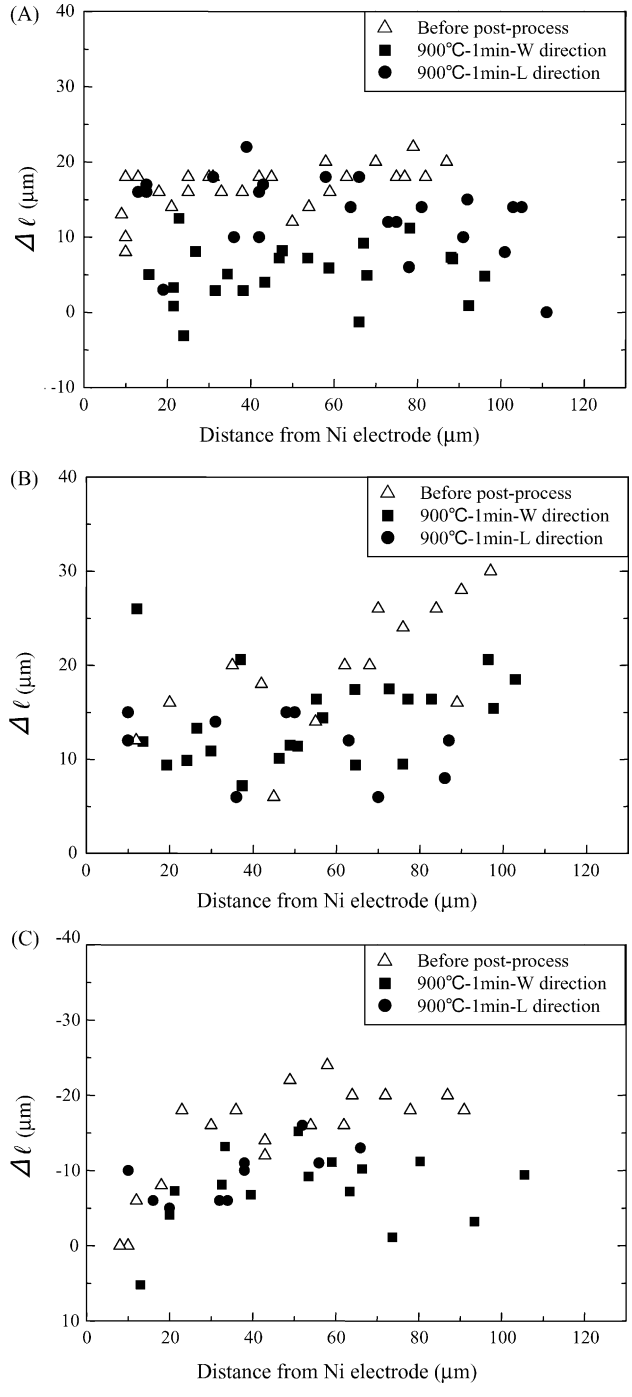

Fig. 5. Difference between crack length created in each direction at each plane after post-process through width and length directions at 900 °C for 1 min: (A) x plane, (B) y plane, and (C) z plane.

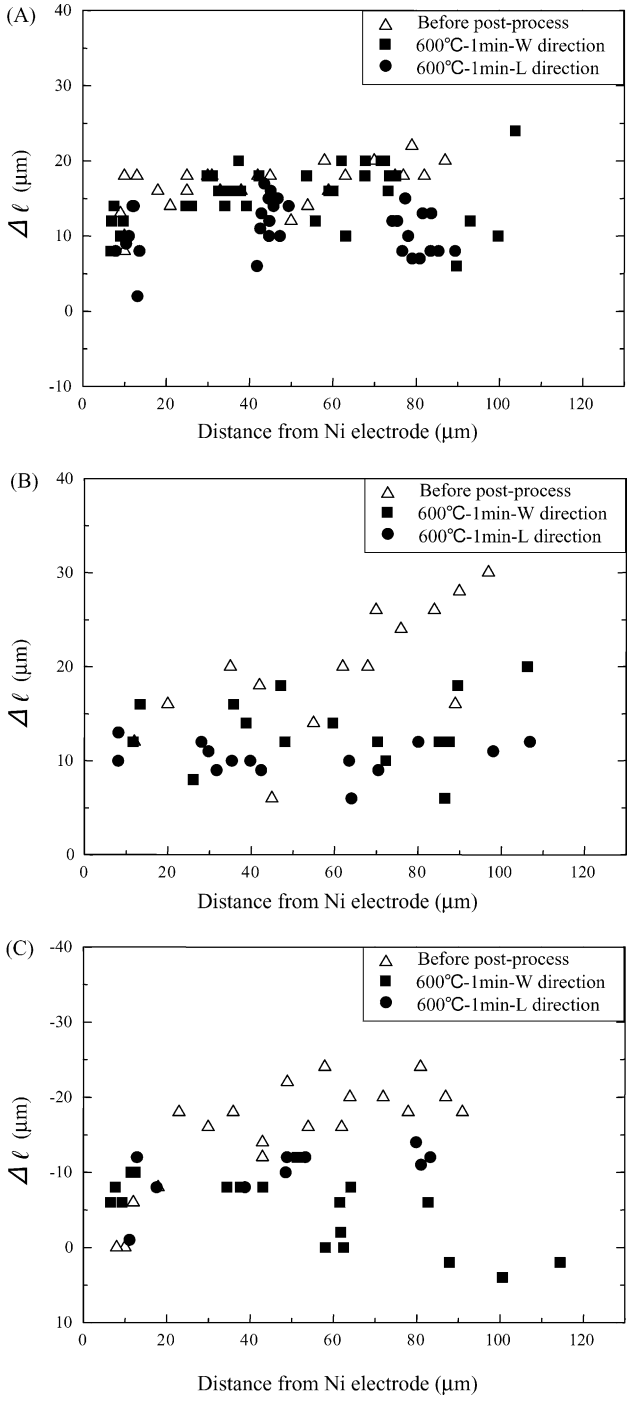

Fig. 6. Difference between crack length created in each direction at each plane after post-process through width and length directions at 600 °C for 1 min: (A) x plane, (B) y plane, and (C) z plane.

14 ± 6 μm at the y plane and -9 ± 4 μm and -8 ± 7 μm at the z plane after the post-process through the length and width directions, respectively. At 600 °C (Fig. 6), the crack length in the x direction at the x plane is longer than that in the z direction, indicating that the stress unbalance still remained. At the y plane, the value of 10 ± 4 μm after the post-process through the length direction is much smaller than that of 21 ± 8 μm before the post-process. The tendency of crack behavior is reversed at the z plane, indicating that the crack length in the z direction is a little longer than that in the y direction. The effect of temperature on the release of stress unbalance is inferior to the x plane in the case of 600 °C.

The difference of the crack length at the x plane is 5 ± 5 μm after the post-process through the width direction at 900 °C, which is much smaller than the crack length of

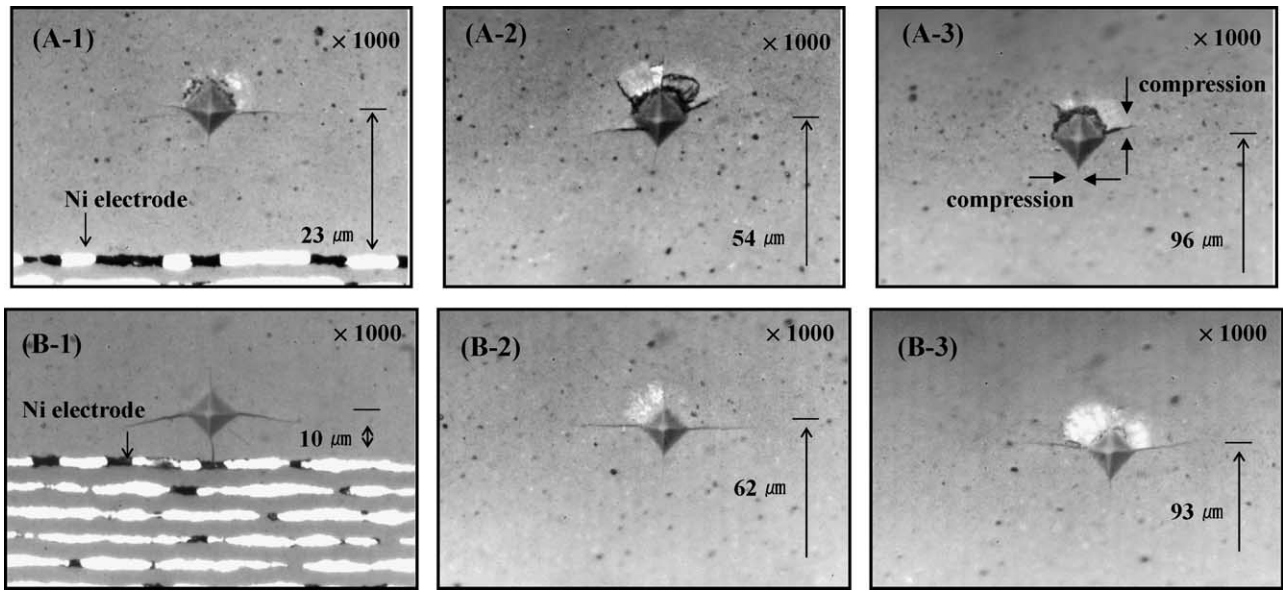

Fig. 7. Micrographs of crack propagation at x plane with distance from electrode after post-process through width direction at 900 °C and 600 °C for 1 min: A and B series are shown as micrographs of crack propagation at 900 °C and 600 °C, respectively.

13 ± 9 μm before the post-process and the crack length at 600 °C. Therefore, higher temperature is more effective in reducing the stress unbalance at the x plane, which can be confirmed with micrographs of crack evolution at different temperatures (600 °C and 900 °C, as shown in Fig. 7). Also, the post-process through the width direction at the x and z planes and the length direction at the y plane indicates its effectiveness in the release of the stress unbalance.

It is evident from Figs. 7 and 8 that the post-process suppresses the crack propagation. Fig. 7 shows the crack formation at the x plane at 900 °C and 600 °C after the post-process through the width direction with the holding time of 1 min. Higher temperature is more effective in crack suppression, indicating that the crack in the z direction is not propagated. The effect of the post-process with increasing the distance from the electrode on crack propagation is not observed, as previously shown in Figs. 2–4. Even though the crack length in the x direction is longer than that in the z direction, the crack length in the x direction after the post-process is similar to the one in the z direction before the post-process. The crack length in the z direction after the post-process is shorter than that in the z direction before the post-process, as already shown in Table 1. This means that the residual tensile stress is almost converted to compressive

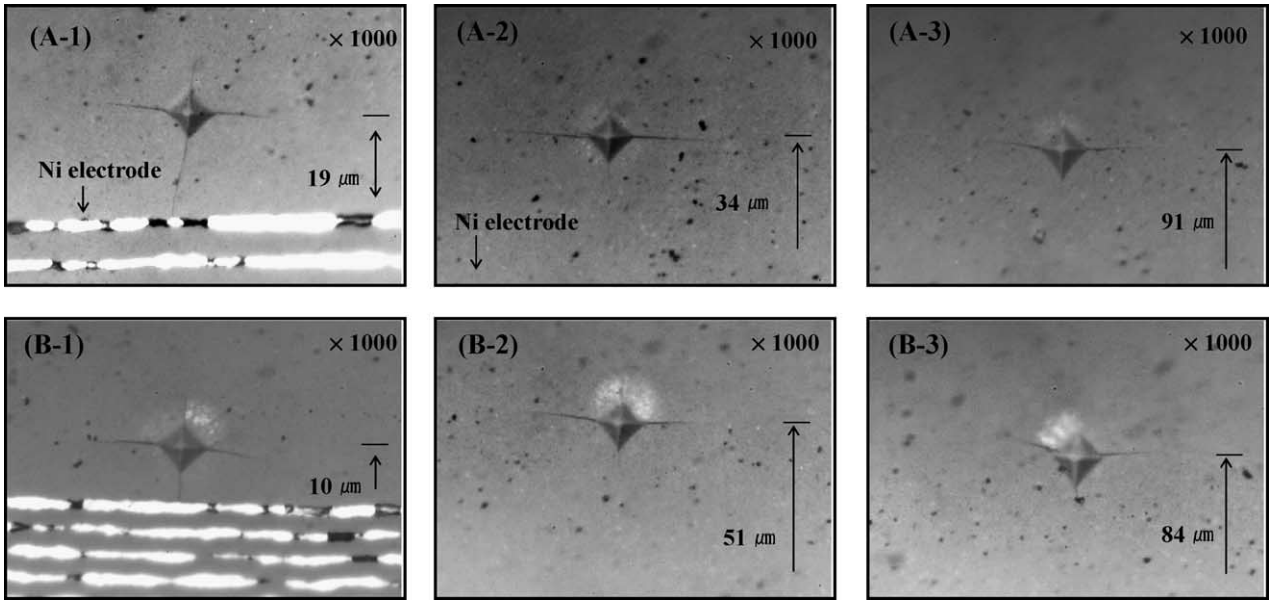

Fig. 8. Micrographs of crack propagation at the x plane with distance form electrode after post-process through length direction at 900 °C and 600 °C for 1 min: A and B series are shown as micrographs of crack propagation at 900 °C and 600 °C, respectively.

stress and the residual compressive stress is enhanced in each direction. The residual stresses in the margins of MLCCs before the post-process indicates that there is the compressive stress of -45 ± 8 MPa in the x direction and the tensile stress of 177 ± 71 MPa in the z direction [7]. Fig. 8 shows the crack formation at the x plane after the post-process through the length direction at 900 °C and 600 °C. The crack formation at 900 °C and 600 °C is very similar to each other. Also, the distance from the electrode does not affect crack formation and propagation in the case of the length direction, showing the stress unbalance with the direction to the electrode. The crack formation through the length direction is very similar to the case of the width direction at 600 °C.

There are two possible explanations for the crack formation in the margins of MLCCs, especially for the difference in crack length with the direction to the lamination and the electrode. One is the difference in the rate of stress formation and relaxation due to the different shrinkage and viscoelastic deformations of constituents. The other is due to the thermal expansion mismatch between dielectric and electrode layers [9,10]. The crack suppression and the stress unbalance release through the post-process could be expected to reduce the stress components induced during the fabrication process, because the heat treatment temperature of 900 °C is very similar to the post-annealing temperature of 950 °C. Therefore, the intrinsic stress components for each case are not much different.

From this study, it is found that the holding time in the post-process does not affect the crack evolution at a heat treatment temperature below the post-annealing temperature. However, the temperature and direction in the post-process play a major role in crack suppression. There are other questions, concerning dielectric properties and microstructural defects after the post-process. These questions are currently under investigation in another studies.

4. Conclusions

The effects of holding time, temperature, and direction on the crack evolution and the release of stress unbalance are investigated in the post-process using pressure and heat treatment. The holding time does not affect the crack suppression except for the x direction at the x plane, indicating that crack length is not affected with the distance from the electrode. Higher temperature is relatively effective in reducing crack length and releasing the stress unbalance at x plane. The width direction is effective in releasing the stress unbalance at the x and z planes, and the length direction is effective at the y plane. Considering the temperature of post-annealing in MLCCs, the results suggest that 900 °C could be the maximum temperature for the post-process. The optimum pressure direction in the post-process is the width direction at the x and z planes and the length direction at the y plane, independent of the holding time.

Acknowledgement

This work has been financially supported by the Korea Institute S & T Evaluation and Planning (KISTEP) through the National Research Laboratory (NRL).

References

[1] G. Arlt, D. Hennigns, G. de With, Dielectric properties of fine-grained barium titanate ceramics, J. Appl. Phys. 58 (1985) 1619–1625.
[2] A.A. Wereszczak, K. Breder, M.K. Ferber, R.J. Bridge, L. Riester, T.P. Kirkland, Failure probability prediction of dielectric ceramics in multilayer capacitors, in: Proceedings of the International Symposium on Multilayer Ceramic Division, Transactions of the AcerS, 100th Annual Meeting and Exhibition of the American Ceramic Society, Cincinnati, OH, 1998.
[3] J. Bergenthal, Mechanical strength properties of multi-layer ceramic chip capacitors, in: 11th Capacitor and Resistor Technology Symposium (CARTS), 1991.
[4] C.R. Koripella, Mechanical behavior of ceramic capacitors, IEEE Trans. Comp. Hybrids Manufact. Technol. 14 (4) (1991) 718–724.
[5] B. Rawal, R. Ladew, R. Garcia, Factors responsible for thermal shock behavior of chip capacitors, in: Proceedings of the 37th Electronic Components Conference, Boston, MA, 1987, pp. 145–156.
[6] G.S. White, C. Nguyen, B. Rawal, Young's modulus and thermal diffusivity measurements of barium titanate based dielectric ceramics, in: Proceedings of Nondestructive Testing of High Performance Ceramics, 1987, pp. 371–379.
[7] D.H. Park, Y.G. Jung, U. Paik, Evaluation of residual stresses in $BaTiO_3$-based Ni-MLCCs with X7R characteristics, J. Mater. Sci. 15 (2004) 253–259.
[8] S.G. Lee, U. Paik, Y.I. Shin, J.W. Kim, Y.G. Jung, Control of residual stresses with post-process in $BaTiO_3$-based Ni-MLCCs, Mater. Des. 24 (3) (2003) 169–176.
[9] G. de With, G. Sweegers, The effect of erosional wear on strength and residual stress during shaping of ceramic multilayer capacitors, Wear 188 (1995) 142–149.
[10] J. Almer, M. Odén, G. Håkansson, Microstructure, stress and mechanical properties of arc-evaporated Cr–C–N coating, Thin Solid Films 385 (2001) 190–197.